Eur. Phys. J. B **23**, 345–350 (2001)

THE EUROPEAN PHYSICAL JOURNAL B

EDP Sciences

Charge profile of surface doped C_{60}

S. Wehrli[1,a], D. Poilblanc[1,2], and T.M. Rice[1]

[1] Theoretische Physik, Eidgenössische Technische Hochschule, 8093 Zürich, Switzerland
[2] Laboratoire de Physique Quantique[b], Université Paul Sabatier, 31062 Toulouse, France

Received 21 June 2001

Abstract. We study the charge profile of a C_{60}-FET (field effect transistor) as used in the experiments of Schön, Kloc and Batlogg. Using a tight-binding model, we calculate the charge profile treating the Coulomb interaction in a mean-field approximation. At low doping, the charge profile behaves similarly to the case of a continuous space-charge layer and becomes confined to a single interface layer for doping higher than ∼0.3 electron (or hole) per C_{60} molecule. The morahedral disorder of the C_{60} molecules smoothens the structure in the density of states.

PACS. 73.25.+i Surface conductivity and carrier phenomena – 73.90.+f Other topics in electronic structure and electrical properties of surfaces, interfaces, thin films, and low-dimensional structures – 74.70.Wz Fullerenes and related materials

Surface doping of high quality organic crystals has recently been achieved by Schön, Kloc and Batlogg [1–3]. This breakthrough has led to novel devices, new superconductors and measurements of transport properties over unprecedented wide ranges of carrier concentration and temperature. A tunable field effect transistor (FET) is used to inject carriers near to the surface of the organic crystal. In this paper we report on calculations of the resulting charge profile. We chose to investigate the case of a C_{60}-crystal which has a special interest in view of the recent observations of superconductivity with a high T_c (∼52 K) in hole doped samples.

The FET used in the work of Schön *et al.* is illustrated in Figure 1a. In the present work, we consider a C_{60} crystal (fcc lattice) with a [001] plane parallel to the gate. Undoped C_{60} is a semiconductor with a 2 eV gap. However, when an electric potential is applied between the gate electrode and the source/drain electrodes, either electrons or holes accumulate on the interface between the C_{60} crystal and the gate dielectric. This leads to a doping of the C_{60} interface planes which allows current to flow parallel to the interface, between the source and the drain. The resistance of this channel can be measured as a function of temperature and doping. The FET can be represented as a planar capacitance with equal and opposite charges on the metal gate and the C_{60} planes near to the interface as shown in Figure 1b. We will calculate the charge profile as a function of the total charge induced at the interface

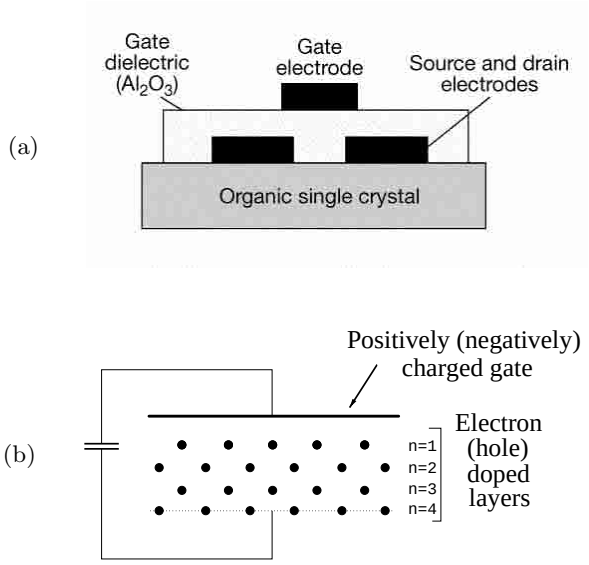

Fig. 1. (a) Schematic picture of the FET as used in the experiments of Schön, Kloc and Batlogg. Picture taken from [1]. (b) Model of the electronic system in the FET.

(or equivalently on the metal gate) rather then in terms of the potential applied to the gate. We limit ourselves to the case of an ideal planar interface with no steps or imperfections.

We begin by introducing a tight-binding model to describe the electronic structure of the C_{60} crystal. The

[a] e-mail: swehrli@itp.phys.ethz.ch
[b] UMR–CNRS 5626

effects of Coulomb interactions are treated within a mean-field (or Hartree) approximation. The resulting density profile gives rise to highly structured density of states (DOS). However we show that the inclusion of morahedral (or orientational) disorder leads to a broadening and suppression of this structure in the DOS.

The C_{60} molecule, which has icosahedral symmetry, is almost spherical. Therefore, in the solid, it orders naturally in the close packed fcc structure. In the following we will assume the (hypothetical) unidirectional structure where all C_{60} molecules have the same orientation [4]. The space group for this structure is $Fm\bar{3}m$ and its primitive cell contains one molecule. The actual low-temperature structure with space group $Pa\bar{3}$ is more complicated and has a unit cell with 4 molecules. However, in the present work, we are interested in the overall charge filling of the layers, for which details of the band structure are unimportant. The lattice constant of the cubic cell (containing 4 molecules) is $a = 14$ Å for pure C_{60} [5]. We introduce here the unit vectors $\boldsymbol{e}_x$, $\boldsymbol{e}_y$ and $\boldsymbol{e}_z$ which span the cubic cell. If one considers only a [001] layer, then the C_{60} molecules form a 2D square lattice. In this case the primitive cell has a side length of $b = \frac{a}{\sqrt{2}} = 10$ Å which is the distance between two neighboring molecules. The 2D primitive cell is spanned by the unit vectors $\boldsymbol{e}_1 = \frac{1}{\sqrt{2}}(\boldsymbol{e}_x + \boldsymbol{e}_y)$ and $\boldsymbol{e}_2 = \frac{1}{\sqrt{2}}(-\boldsymbol{e}_x + \boldsymbol{e}_y)$.

The kinetic energy is well described by a tight-binding Hamiltonian with nearest neighbor (n.n.) hopping [4,6]:

$$H_{\mathrm{TB}} = \sum_{\langle nj\alpha, n'j'\alpha'\rangle} t_{\alpha'\alpha}(\boldsymbol{\delta})\; c^{\dagger}_{n'j'\alpha'}\; c_{nj\alpha}, \qquad (1)$$

where $t_{\alpha'\alpha}(\boldsymbol{\delta})$ are the hopping integrals depending on the relative position $\boldsymbol{\delta}$ of neighboring molecules. The label n denotes the different layers starting with the $n = 1$ layer closest to the gate. Within a layer n, the different sites are labelled by the index j. Finally, the index α denotes the different orbitals of the C_{60} molecule. The brackets $\langle\rangle$ indicate a summation over n.n. only. Summation over spin degrees of freedom is implicitly assumed. Hamiltonian (1) is invariant under translations parallel to the $z = 0$ plane and can partly be diagonalized in the 2D k-space:

$$H_{\mathrm{TB}} = \sum_{\boldsymbol{k}} \sum_{n\alpha, n'\alpha'} H_{n'\alpha', n\alpha}(\boldsymbol{k})\; c^{\dagger}_{n'\alpha'}(\boldsymbol{k})\; c_{n\alpha}(\boldsymbol{k}), \qquad (2)$$

where $|n - n'| \leq 1$ and $\boldsymbol{k}$ is the two-dimensional wavevector parallel to the planes. In the case of the conduction band, the structure of the hopping integrals $t_{\alpha'\alpha}(\boldsymbol{\delta})$ are given by the t_{1u} symmetry of the LUMO (Lowest Unoccupied Molecular Orbital) which is threefold degenerate [6]. The corresponding wave-functions can be chosen such as to transform as x, y and z under the icosahedral symmetry group which reduces the number of independent hopping integrals to 4. They are given in Table 1. The matrix elements $H_{n'\alpha', n\alpha}(\boldsymbol{k})$ in (2) can be calculated

Table 1. Hopping integrals (in meV) for hopping in the $\boldsymbol{\delta} = (110)$ direction of the $[\boldsymbol{e}_x\boldsymbol{e}_y\boldsymbol{e}_z]$ coordinate system. The sign of t_{xy} changes for hopping in the $(1\bar{1}0)$ direction. Hopping integrals in other directions follow from rotations around the threefold (111) axes. Numerical values were taken from [4] and adjusted by a factor 1.11 for a lattice constant $a = 14.0$ Å of pure C_{60}.

	$\|x\rangle$	$\|y\rangle$	$\|z\rangle$
$\langle x\|$	$t_{xx} = 5.5$	$\pm t_{xy} = -27.8$	0
$\langle y\|$	$\pm t_{xy} = -27.8$	$t_{yy} = 41.8$	0
$\langle z\|$	0	0	$t_{zz} = -23.5$

explicitly which yields for intraplanar processes ($n' = n$),

$$\begin{aligned} H_{nx,nx}(\boldsymbol{k}) &= 2t_{xx}[\cos(k_1 b) + \cos(k_2 b)], \\ H_{ny,ny}(\boldsymbol{k}) &= 2t_{yy}[\cos(k_1 b) + \cos(k_2 b)], \\ H_{nx,ny}(\boldsymbol{k}) &= 2t_{xy}[\cos(k_1 b) - \cos(k_2 b)], \\ H_{nz,nz}(\boldsymbol{k}) &= 2t_{zz}[\cos(k_1 b) + \cos(k_2 b)], \end{aligned} \qquad (3)$$

and for interplanar processes ($n' = n + 1$),

$$\begin{aligned} H_{n+1x,nx}(\boldsymbol{k}) &= 2t_{yy}\cos[(k_1{-}k_2)b/2]{+}2t_{zz}\cos[(k_1{+}k_2)b/2], \\ H_{n+1y,ny}(\boldsymbol{k}) &= 2t_{zz}\cos[(k_1{-}k_2)b/2]{+}2t_{xx}\cos[(k_1{+}k_2)b/2], \\ H_{n+1z,nz}(\boldsymbol{k}) &= 2t_{xx}\cos[(k_1{-}k_2)b/2]{+}2t_{yy}\cos[(k_1{+}k_2)b/2], \\ H_{n+1x,nz}(\boldsymbol{k}) &= \mathrm{i}\,2t_{xy}\sin[(k_1 - k_2)b/2], \\ H_{n+1y,nz}(\boldsymbol{k}) &= \mathrm{i}\,2t_{xy}\sin[(k_1 + k_2)b/2]. \end{aligned} \qquad (4)$$

The band structure and DOS of a single layer (interplanar processes are turned off) are shown in Figure 2. As a comparison, the 3D DOS is shown as well. The logarithmic van-Hove singularities are clearly apparent in the DOS. Moreover, one observes a symmetric DOS. This is explained by the substitution $\boldsymbol{k} \to \boldsymbol{k} + (\frac{\pi}{b}, \frac{\pi}{b})$ which leads to $H \to -H$ for the one-layer Hamiltonian (3). It implies also that all bands at $(\frac{\pi}{2b}, \frac{\pi}{2b})$ cross at zero energy. Coupling to neighboring layers breaks this symmetry. The structure of the hopping integrals for the valence band are somewhat more complicated due to the fivefold degeneracy of the HOMO (Highest Occupied Molecular Orbital) with h_u symmetry. They are described in detail in reference [6] and similar matrix elements as in (3) and (4) were calculated with parameters taken from [6].

The Coulomb interaction can be included by adding the following term to the tight-binding Hamiltonian (1),

$$\begin{aligned} H_{\mathrm{Coul}} = &\sum_{nj\alpha} U_{\mathrm{Gate}}(n) n_{nj\alpha} \\ &+ \frac{1}{2} \sum_{nj\alpha, n'j'\alpha'} V_{ee}(nj, n'j') n_{nj\alpha} n_{n'j'\alpha'}, \end{aligned} \qquad (5)$$

where $n_{nj\alpha}$ is the number operator. The first term is the potential due to the positive charge on the gate. The second term is the electron-electron Coulomb repulsion. Here we follow Antropov *et al.* [7] by using a screened Coulomb interaction for electrons on different sites and an on-site

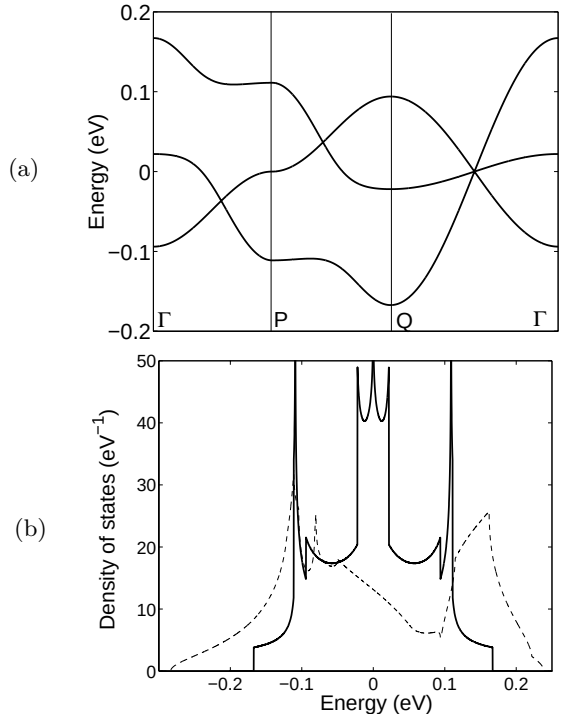

Fig. 2. (a) C_{60} conduction band of the 2D square lattice. The coordinates of the high-symmetry points in the Brillouin zone are $\Gamma(0,0)$, P$(\frac{\pi}{b},0)$,Q$(\frac{\pi}{b},\frac{\pi}{b})$. (b) DOS per C_{60} and for both spins. *Solid line:* 2 dimensions. *Dashed line:* 3 dimensions.

interaction U_0 for electrons on the same site,

$$V_{ee}(nj,n'j') = \begin{cases} U_0 & \text{if} \quad \boldsymbol{R}_{nj} = \boldsymbol{R}_{n'j'} \\ \frac{e^2}{\varepsilon\left|\boldsymbol{R}_{nj}-\boldsymbol{R}_{n'j'}\right|} & \text{if} \quad \boldsymbol{R}_{nj} \neq \boldsymbol{R}_{n'j'} \end{cases}, \quad (6)$$

with ε being the dielectric constant of C_{60} and $\boldsymbol{R}_{nj}$ denoting the positions of the sites. Note that this interaction does not distinguish between different orbitals. The dielectric constant ε and the on-site interaction U_0 are easily accessible in the literature. We use the experimental estimation of $\varepsilon = 4.4$ by Hebard *et al.* [8] and the theoretical value of $U_0 = 1$ eV by Antropov *et al.* [7]. Somewhat different values of $\varepsilon = 3.66$ and $U_0 = 1.27$ eV are proposed from theoretical calculations by Pederson *et al.* [9].

The full Hamiltonian including the Coulomb term is a complicated many-body problem. We solve it within the mean-field approximation. From symmetry, solutions should be invariant under translations parallel to the planes. The mean-field charge distribution and the resulting potential are then independent of the in-plane site position j and the wave-functions can be decomposed as

$$\Psi_{\nu\boldsymbol{k}}(nj\alpha) = \frac{1}{\sqrt{N_2}} \mathrm{e}^{\mathrm{i}\boldsymbol{R}^{\square}_{nj}\boldsymbol{k}} \psi_{\nu\boldsymbol{k}}(n\alpha), \quad (7)$$

where ν is a band index and $\boldsymbol{R}^{\square}_{nj}$ is the inplane component of $\boldsymbol{R}_{nj}$. $N_{\square}$ is the number of sites per layer. For a fixed $\boldsymbol{k}$, the perpendicular part $\psi_{\nu\boldsymbol{k}}(n\alpha)$ of the wave-function is the solution of a Schrödinger equation with a partly discrete spectrum $\{E_{\nu\boldsymbol{k}}\}$. In the mean-field approximation, every occupied electronic $\nu\boldsymbol{k}$ state contributes $\left|\psi_{\nu\boldsymbol{k}}(n\alpha)\right|^2 / N_{\square}$ electrons to each orbital α in layer n. The sum over all these contributions leads, at zero temperature, to the electron distribution

$$\rho(n) = \frac{2}{N_{\square}} \sum_{E_{\nu\boldsymbol{k}}<E_{\mathrm{F}}} \sum_{\alpha} \left|\psi_{\nu\boldsymbol{k}}(n\alpha)\right|^2, \quad (8)$$

where $\rho(n)$ is the total number of electrons per site in layer n. The factor 2 comes from the spin degrees of freedom. Within the mean-field approximation, the Coulomb part (5) can be written as $H^{\mathrm{MF}}_{\mathrm{Coul}} = \sum_{nj\alpha} U_{\mathrm{MF}}(n) n_{nj\alpha}$ where

$$U_{\mathrm{MF}}(n) = U_{\mathrm{Gate}}(n) + \sum_{n'j'} \rho(n')\, V_{ee}(nj,n'j'). \quad (9)$$

The sum in the second term as well as the potential created by the gate are divergent. However, these divergences cancel when the overall system is neutral. In order to make this more explicit, we add and subtract a hypothetical potential created by uniformly charged layers whose total charge equals the actual charge of the C_{60} layers. The mean-field potential can then be rewritten as a sum of two terms

$$U_{\mathrm{MF}}(n) = U_{\mathrm{Cap}}(n) + U_{\mathrm{Corr}}(n). \quad (10)$$

The first term, U_{Cap}, is given by the superposition of a series of planar capacitance formed by the negative charge $-e\rho(n')$ on each layer n' combined with the corresponding positive charge $+e\rho(n')$ on the gate. Choosing $U_{\mathrm{Cap}}(1) = 0$ yields

$$U_{\mathrm{Cap}}(n) = \frac{4\pi e^2}{\varepsilon\sqrt{2}b} \sum_{n'} \rho(n')\,[\min(n,n') - 1], \quad (11)$$

where it has to be distinguished whether the given layer n lies inside or outside the capacitance with charges $\pm e\rho(n')$. Using $\varepsilon = 4.4$ and $b = 10$ Å leads to a prefactor $4\pi e^2/\varepsilon\sqrt{2}b = 2.9$ eV. The second part of the mean-field potential, U_{Corr}, includes the corrections arising from the discreteness of the charge distribution and is given by

$$U_{\mathrm{Corr}}(n) = \sum_{n'} \rho(n')\, V_{\mathrm{Corr}}(|n-n'|) \quad \text{with} \quad (12)$$

$$V_{\mathrm{Corr}}(|n-n'|) = \sum_{j'} V_{ee}(nj,n'j') - \int \frac{\mathrm{d}^2 R_{n'}\, e^2}{b^2\, \varepsilon\, |\boldsymbol{R}_n - \boldsymbol{R}_{n'}|},$$

where b^2 is the surface of the two-dimensional unit cell and $\boldsymbol{R}_n$ lies in the plane n. In equation (12) we expect the largest corrections for $n' = n$ since the difference of the potential created by a uniformly and a discretely charged plane is only sizeable at short distance. V_{Corr} cannot be expressed analytically since it involves an infinite sum over a two-dimensional lattice. The result from numerical summation is given in Table 2. The function $V_{\mathrm{Corr}}(\Delta n = |n-n'|)$ is rapidly decreasing and we will only retain the $\Delta n = 0$ term in the following. The correction term then becomes

$$U_{\mathrm{Corr}}(n) = -\rho(n) \left(3.9 \frac{e^2}{\varepsilon b} - U_0 \right). \quad (13)$$

Table 2. The function $V_{\rm Corr}(\Delta n)$ as calculated by numerical summation.

$\Delta n = \lvert n - n' \rvert$	$V_{\rm Corr}(\Delta n)$ (eV)
0	$U_0 - 3.90\, e^2/\varepsilon b = U_0 - 1.28 = -0.28$
1	$-0.042\, e^2/\varepsilon b = -0.014$
2	$-10^{-3}\, e^2/\varepsilon b = -3 \times 10^{-4}$

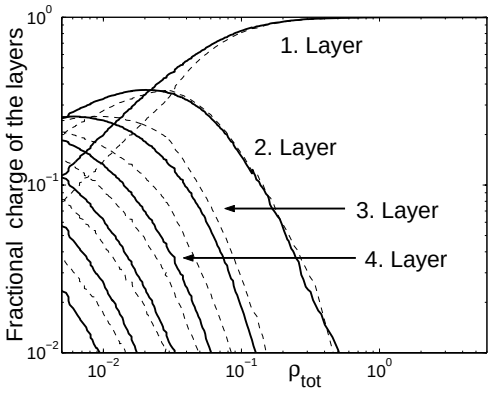

Fig. 3. Relative charging of the first layers as a function of total charge in the system (per area of the 2D unit cell). Both axis are in logarithmic units. *Solid line:* Conduction band. *Dashed line:* Valence band.

In fact, the second part of this correction overestimates the on-site interaction U_0. The contribution of this term is proportional to $\rho(n)$ which reflects the fact that an electron feels its own mean-field. This is an artifact of the mean-field approximation. In order to improve our model, we require that the on-site interaction should only be effective when there is more than one electron on the molecule ($\rho(n) > 1$), leading to the correction term

$$U_{\rm Corr}(n) = -3.9\frac{e^2}{\varepsilon b}\rho(n) + U_0 \max[0, \rho(n) - 1]. \qquad (14)$$

The mean-field Hamiltonian was solved self-consistently at zero temperature by numerical means. The mean-field potential (10) was used with the correction term (14). The resulting charge profile as a function of total charge is shown in Figure 3. We have done the calculation for both, conduction and valence band, which led to similar results. In the following we focus on the conduction band. It can be seen that more than 98% of the total charge is confined to the first layer for doping higher than $\rho_{\rm tot} = 0.3$. Furthermore the confinement to the interface increases with the total charge. The mean distance of the charge distribution from the interface is defined as $z_0 = \sum_{n\geq 1} n\, d\, \rho(n)/\rho_{\rm tot}$, where $d = 7$ Å is the width of one layer. For $\rho_{\rm tot} < 0.1$, this mean distance is found to follow a power law given by $z_0[\text{Å}] \approx 3.8\, \rho_{\rm tot}^{-1/3}$ with $\rho_{\rm tot}$ in units of particles per area of the 2D unit cell. This power law behavior with respect to $\rho_{\rm tot}$ is identical to the case of a standard space-charge layer in a continuous medium [10], which predicts $z_0[\text{Å}] = 3.02\ (\rho_{\rm tot}\, m_z/\varepsilon)^{-1/3} = 5.08\ \rho_{\rm tot}^{-1/3}$, where the effective mass (perpendicular to the interface) of the bulk conduction band minima (X(1,0,0) points) is estimated

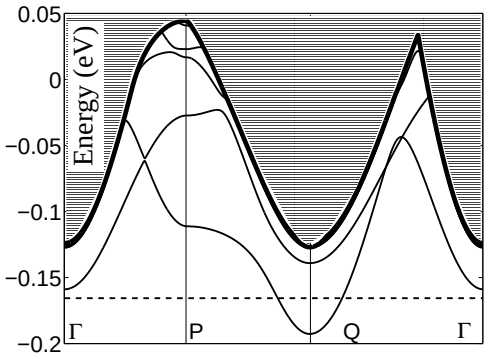

Fig. 4. *Solid lines:* Conduction bands below the continuous spectrum for $\rho_{\rm tot} = 0.1$. *Bold solid line:* Onset of the continuous spectrum. *Dashed line:* Fermi energy.

to be $m_z = 0.92\, m_{\rm e}$ [4,6]. However, it is important to notice that our microscopic calculation gives a different prefactor. In addition, z_0 tends to saturate for $\rho_{\rm tot} > 0.1$, a regime that cannot be understood in the continuum model. In order to test the role of the correction term, we repeated the same calculation with $U_{\rm MF} = U_{\rm Cap}$, *i.e.* for uniformly charged planes. This led to a somewhat weaker confinement at high doping (∼10% less charge on the first layer for $\rho_{\rm tot} = 1$). At low doping the effect of $U_{\rm Corr}$ vanishes because the charge is distributed over several layers. Knowing the charge profile and hence $U_{\rm MF}(n)$, the band structure can be calculated. Figure 4 shows the conduction band for $\rho_{\rm tot} = 0.1$. Few bands lie below the continuous spectrum and only the lowest of the 3 LUMO-bands is occupied in the region of the Q-point. In Figure 5a the evolution of the discrete states at Q is shown as a function of doping. One observes that the Fermi level is always below the bottom of the continuous spectrum. This is true in general and reflects the fact that all electrons are bound to the interface since the overall system is neutral. Furthermore, only the lowest band is occupied at low doping which is again consistent with theory of space-charge layers [10]. Of course, at doping higher than $\rho_{\rm tot} \approx 2$ the second LUMO-band has to be filled as well. In addition, we note that the continuous spectrum shifts up sharply as the total charge increases. Therefore, at doping higher than $\rho_{\rm tot} \approx 0.3$, the first layer becomes essentially decoupled from the continuous states of the subsequent layers. The energy levels at Q remain constant and the dispersion is given by the LUMO-bands of a single, isolated layer (Fig. 2a). The decoupling effect is due to the correction term (14) which drastically shifts the energy of the first layer with respect to the second one. If this term is omitted, as shown in Figure 5b, then the bottom of the continuous spectrum follows roughly the Fermi energy and the decoupling of the first layer is much less effective.

In A_3C_{60}, a scaling of the superconducting $T_{\rm c}$ with increasing lattice constant and hence with the DOS is observed [11]. However, the sharp peaks of the 2D DOS (Fig. 2b) are not reflected in the behavior of $T_{\rm c}$ as measured by Schön *et al.* [1]. A possible explanation for this is the morahedral disorder which is considered in the following for the case of a single 2D layer.

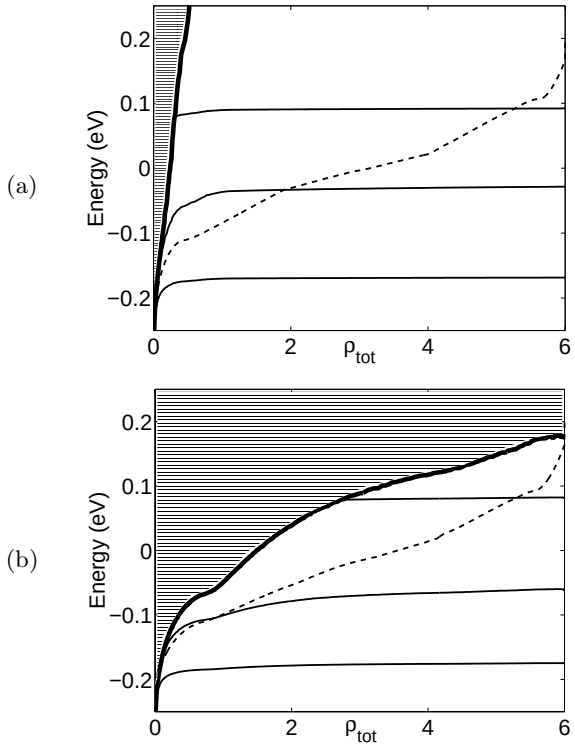

Fig. 5. (a) *Solid lines:* Discrete levels at Q as a function of $\rho_{\rm tot}$. *Bold solid line:* Bottom of the continuous spectrum. *Dashed line:* Fermi energy. (b) As (a), but without correction term $U_{\rm Corr}$.

The rotational motion of a C_{60} molecule in a crystal is described by a potential in the three Euler angle coordinates. This potential has, in addition to an absolute minimum, a local minimum which is only $\Delta = 11$ meV higher and corresponds to a non-equivalent orientation of the molecule [12]. Therefore, C_{60} molecules can flip into the second orientation causing the so-called morahedral disorder. The ratio between the number of flipped and unflipped molecules is given by a Boltzmann factor $\exp(-\Delta/kT)$. However, a freezing in is observed at 85 K. Below this temperature the crystal is in a glass phase with 15% of the molecules being flipped. If the problem is considered from a tight-binding point of view, then one expects the hopping integrals to be different for hopping between inequivalently oriented molecules. Hence, one gets a tight-binding model where different hopping integrals are distributed randomly. This will suppress structure in the DOS, as was calculated by Gelfand and Lu in the case of bulk C_{60} [13]. Here, we consider the effect of morahedral disorder on the DOS of a single electron-doped [001] layer. The two types of inequivalent orientations lead to two sets of LUMO wave-functions. We shall denote the new ones on flipped molecules as $|\tilde{x}\rangle$, $|\tilde{y}\rangle$ and $|\tilde{z}\rangle$. These two sets can be related by a 90-degree rotation around the z-axes. The hopping integrals between inequivalently oriented molecules are given in Table 3. In order to calculate the DOS of the disordered system we set up a finite, two dimensional system which could be diagonalized exactly (for non-interacting electrons). The resulting DOS is shown in Figure 6. The van-Hove singularities are washed out, but a rather sharp peak remains at the center of the band.

Table 3. Hopping integrals (in meV) for hopping from an unflipped to a flipped molecule in the (110) direction of a fcc lattice. The new (tilded) wave-functions were ordered according to their parity. Note that the sign of $\tilde{t}_{xx}$ and $\tilde{t}_{yy}$ change for hopping in the $(1\bar{1}0)$ direction. Numerical values were taken from [13] and adjusted by a factor 11 as proposed by Gelfand and Lu.

	$\lvert x\rangle$	$\lvert y\rangle$	$\lvert z\rangle$
$\langle\tilde{y}\rvert$	$\tilde{t}_{xy} = 22.9$	$\pm\tilde{t}_{yy} = 40.8$	0
$\langle\tilde{x}\rvert$	$\pm\tilde{t}_{xx} = 19.2$	$\tilde{t}_{xy} = 22.9$	0
$\langle\tilde{z}\rvert$	0	0	$\tilde{t}_{zz} = -29.4$

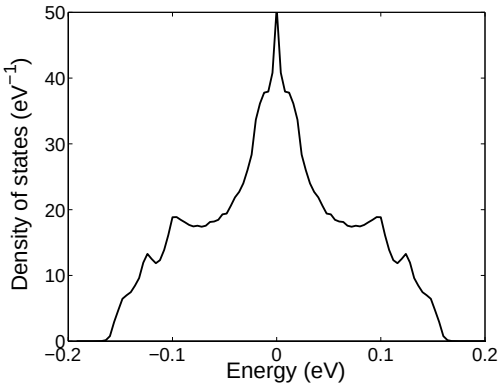

Fig. 6. DOS for a disordered 50×50 site lattice and a flipping ratio of 15%. The statistical average over 200 disorder configurations was taken.

In conclusion, we have investigated the electronic properties of surface doped C_{60}. The charge profile was calculated as a function of total charge in the system and it was found that the charge accumulation on the first layer increases with the total charge. At high doping, above $\sim$0.3 electron per molecule, the first layer becomes essentially decoupled from the subsequent layers. This suggests that the electronic system should be well described by a single layer in this regime. In particular, the relevant DOS is then the one of a two dimensional system and hence substantially higher than in the bulk. Having chosen the unidirectional structure (one orientation per primitive cell), we found maximal values of the DOS near the center of the band. Introducing morahedral disorder led to a smoothened DOS which still shows a peak at half filling, *i.e.* in the region where Schön *et al.* measure the maximum $T_{\rm c}$.

We thank B. Batlogg for fruitful discussions throughout this work. D.P. also acknowledges support from the Center for Theoretical Studies and from the Physics Department at ETH-Zürich.

References

1. J.H. Schön, Ch. Kloc, B. Batlogg, Nature **408**, 549 (2000).
2. J.H. Schön, Ch. Kloc, B. Batlogg, Nature **406**, 702 (2000).
3. J.H. Schön, Ch. Kloc, R.C. Haddon, B. Batlogg, Science **288**, 656 (2000).
4. S. Satpathy, V.P. Antropov, O.K. Andersen, O. Jepsen, O. Gunnarsson, A.I. Liechtenstein, Phys. Rev. B **46**, 1773 (1992).
5. S. Liu, Y.-J. Lu, M.M. Kappers, J.A. Ibers, Science **254**, 408 (1991).
6. N. Laouini, O.K. Andersen, O. Gunnarsson, Phys. Rev. B **51**, 17446 (1995).
7. V.P. Antropov, O. Gunnarsson, O. Jepsen, Phys. Rev. B **46**, 13647 (1992).
8. A.F. Hebard, R.C. Haddon, R.M. Fleming, A.R. Kortan, Appl. Phys. Lett. **59**, 2109 (1991).
9. M.R. Pederson, A.A. Quong, Phys. Rev. B **46**, 13584 (1992).
10. T. Ando, A.B. Fowler, F. Stern, Rev. Mod. Phys. **54**, 437 (1982).
11. O. Gunnarsson, Rev. Mod. Phys. **69**, 575 (1997).
12. W.I.F. David, R.M. Ibberson, T. Matsuo, Proc. R. Soc. Lond. A **442**, 129 (1993).
13. M.P. Gelfand, J.P. Lu, Phys. Rev. Lett. **68**, 1050 (1992).